



Short communication

Superior hydrogen storage and electrochemical properties of Mg–La–Pd trilayer films at room temperature



Tong Liu ^{a,*}, Yurong Cao ^a, Hui Li ^a, Wusheng Chou ^b, Xingguo Li ^{c,1}

^a Key Laboratory of Aerospace Materials and Performance (Ministry of Education), School of Materials Science and Engineering, Beihang University, Beijing 100191, China

^b School of Mechanical Engineering and Automation, Beihang University, Beijing 100191, China

^c Beijing National Laboratory for Molecular Sciences (BNLMS), The State Key Laboratory of Rare Earth Materials Chemistry and Applications, College of Chemistry and Molecular Engineering, Peking University, Beijing 100871, China

HIGHLIGHTS

- We prepared a series of Mg–La–Pd trilayer films by magnetron sputtering method.
- The La 3 nm film possessed the fastest sorption rate compared with other films.
- The hydrogenation of the La 3 nm film saturated within 14 s at 298 K.
- The La 3 nm film released 80% of hydrogen within 60 min at 298 K.
- The maximum discharge capacity of the La 3 nm film was 377.8 mAh g⁻¹.

ARTICLE INFO

Article history:

Received 26 January 2014

Received in revised form

18 April 2014

Accepted 20 May 2014

Available online 2 June 2014

Keywords:

Magnetron sputtering

Thin film

Hydrogen storage

Electrochemical properties

ABSTRACT

A series of Mg–La–Pd trilayer films (La = 0.5–9 nm) have been prepared by magnetron sputtering method. When the thickness of La layer is larger than 3 nm, the distribution of La element becomes homogeneous. The hydrogen storage properties of the films under 0.1 MPa H₂ and at 298 K are investigated by measuring their resistance and optical transmittance during the hydrogenation. The hydrogenation of the La 3 nm film saturates within 14 s and possesses the fastest absorption kinetics compared with other Mg–La–Pd films. The further increase of La thickness decreases the hydrogenation rate due to the decreased hydrogen diffusion rate through this layer. The La 3 nm film also exhibits the fast hydrogen desorption rate in air at room temperature. It releases 80% of hydrogen within 60 min. The electrochemical properties of the Mg–La–Pd films have been carried out in 6 M KOH with a three-electrode cell. Among these films, the La 3 nm film possesses the largest anodic area and anodic peak current, as well as the highest maximum discharge capacity of 377.8 mAh g⁻¹.

© 2014 Elsevier B.V. All rights reserved.

1. Introduction

In recent years, extensive research has been focused on various potential hydrogen storage materials [1,2]. Among numerous hydrogen storage materials, magnesium and magnesium based materials have attracted great attention because of their high theoretical hydrogen storage capacities (7.6 mass% for MgH₂), lightweight and low cost [3–6]. However, the slow kinetics and

high desorption temperature of the Mg-based materials seriously impede their applications [7]. Recently, tremendous efforts have been devoted to overcome these drawbacks, such as the fabrication of Mg-based nanocomposites [8], the addition of alloying elements and catalytic components [9,10], and the surface modification [11].

The Mg-based films prepared by sputtering, thermal evaporation and other methods exhibit obvious advantages because their dimension and crystallinity can be accurately tailored in nanoscale [12–16]. These thin films show potential utilization as a hydrogen detecting sensor [17,18]. The effects of the thickness and microstructure of these films on the hydrogen absorption and desorption kinetics have been investigated [19–26]. Xu et al. [21] demonstrated that Mg_{2-x}Al_x/Ni films exhibited superior hydrogen

* Corresponding author. Tel.: +86 10 8231 6192; fax: +86 10 8231 4869.

E-mail addresses: tongliu@buaa.edu.cn (T. Liu), xgli@pku.edu.cn (X. Li).

¹ Tel.: +86 10 6275 3691; fax: +86 10 6276 5930.

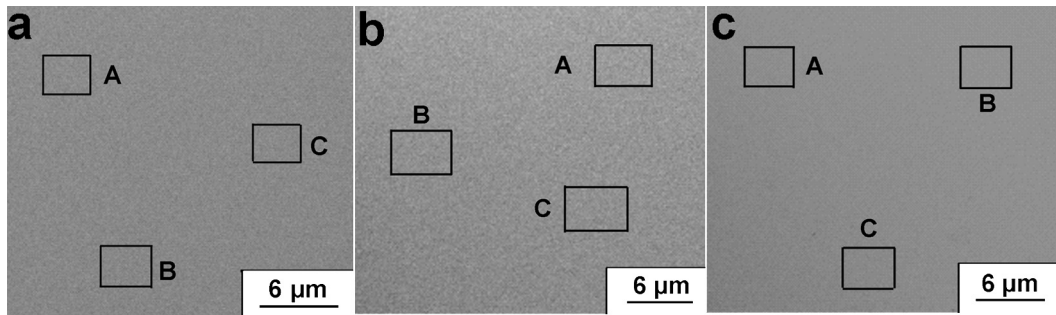


Fig. 1. The SEM images of the Mg–La–Pd trilayer films, (a) La 0.5 nm sample, (b) La 2 nm sample, (c) La 3 nm sample. The EDS measurements were conducted at A, B and C areas.

absorption and desorption performance. Xin and coworkers [27] prepared Mg/Al/Pd trilayer films and found that the hydrogen storage properties of Mg/Pd films could be significantly improved with the addition of Al interlayer. Mitlin et al. [28] reported that Mg–Fe–Ti films were capable of absorbing nearly 5 wt. % H₂ in seconds and desorbing in minutes, and this sorption behavior was stable over cycling. Rare earth elements such as La are known as effective catalysts. Slattery reported that La₂Mg₁₇ can absorb 3.1 wt. % H₂ at 623 K with LaH₃ acting as a catalyst [29]. Li studied the maximum discharge capacity of the La/Ni/Al film, which was only about 220 mAh g⁻¹ [30]. To the best of our knowledge, Mg-based films doped with rare earth element have rarely been investigated. Furthermore, the electrochemical properties of Mg-based films were rarely reported. In this study, we intend to prepare a series of Mg–La–Pd thin films with various thickness of La interlayer by magnetron sputtering, and study the effect of the La interlayer on their properties. The Pd cap layer is necessary to protect Mg and La from oxidation. The hydrogenation/dehydrogenation properties of these thin films under mild condition were systematically investigated by measuring the changes in the electric resistance and the optical transmittance value during hydrogen sorption. In addition, the electrochemical hydrogen storage properties of these samples were further studied using three-electrode system.

2. Experimental

The Mg–La–Pd trilayer films with various thicknesses of the La interlayer were prepared using the direct current (DC) magnetron sputtering system with the background pressure of about 2×10^{-4} Pa. The magnetron discharges were generated under an argon pressure of 0.6 Pa with the argon flow rate of 76 sccm. The purity of the argon is 99.999%. The discharge powers of Mg, La and Pd were 14, 24 and 45 W, respectively. The deposition rates of Mg, La and Pd were measured to be 0.178, 0.05 and 0.33 nm s⁻¹, respectively. Firstly, Mg layers of 100 nm were deposited onto Si (110) wafers and glass substrates using a Mg (99.99%) target. Then, La layers of 0.5 nm, 2 nm, 3 nm, 4.5 nm and 9 nm were deposited on the Mg films, respectively, using La (99.99%) target. Finally, a Pd layer of 10 nm was coated on top of the La layer using Pd (99.99%) target. Samples with different La thicknesses of 0.5, 2, 3, 4.5 and 9 nm are referred to as La 0.5 nm, La 2 nm, La 3 nm, La 4.5 nm and La 9 nm, respectively.

The crystal structures of these samples were identified by power X-ray diffraction (XRD) using a Rigaku X-ray diffractometer with monochromatic Cu K α radiation. The changes in resistance of these films were recorded in a gas loading cell equipped with a four-probe resistance measurement setup and monitored using an Agilent 34401A digital multimeter. The electrochemical experiments were performed at room temperature in 6 M KOH with a

three-electrode cell using electrochemical workstation (CHI660E). Platinum foil and Hg/HgO were used as the counter and reference electrode, respectively. Prior to the measurements, the films were subjected to an activation procedure between -1.2 and 0.45 V (versus Hg/HgO) at a scan rate of 0.05 V s⁻¹. This potential range corresponds to the Pd(OH)₂ formation/removal on the Pd cap layer. During the charge/discharge measurement, the electrodes rest for 300 s before they are charged at 16438 mA g⁻¹ for 2400 s. Then, the electrodes rest for another 300 s, and are discharged at 3287 mA g⁻¹. The cut-off voltage for the discharge process was 0 V. The discharge capacity of each sample was measured for 100 cycles.

3. Results and discussion

Fig. 1 shows the SEM images of Mg–La–Pd thin films, and the compositions (at.%) of these thin films at A, B and C areas were measured by EDS and listed in **Table 1**. It is found that for the La 0.5 nm sample, the La content at area A is 0, quite different from the La contents at area B (2.8 at.%) and C (2.7 at.%). It can be concluded that the La layer in the La 0.5 nm sample is discontinuous. As to the La 2 nm sample, the La contents at areas A, B and C are 1.2, 2.5 and 3.7 at.%, respectively, indicating that the distribution of La element in the La 2 nm sample is uneven. It is noted that for the La 3 nm sample, the La contents at areas A, B and C are 4.0, 3.9 and 4.0 at.%, respectively. This implies that when the thickness of La is larger than 3 nm, the distribution of La element in the Mg–La–Pd films becomes homogeneous.

The electrical resistance of the Mg-based film changes during the hydrogen absorption, which provides the information of the hydrogenation kinetics [31]. The time evolution of the relative resistance, R/R_0 , of the Mg–La–Pd films under 0.1 MPa H₂ at 298 K is shown in **Fig. 2**, where R_0 and R are the initial resistance and measured resistance of the film during hydrogenation, respectively. The slope of the curve before reaching a saturation value reflects the hydrogenation rate of the films. All the samples except La 9 nm and La 4.5 nm exhibit a significant increase in relative resistance change after exposure to hydrogen. It is found that with the increase of the La thickness from 0.5 to 3 nm, the hydrogenation rate rises. La 3 nm film demonstrates the fastest hydrogen absorption kinetics at ambient temperature among these samples. The relative resistance of La 3 nm sample reaches a constant value within only

Table 1
The compositions (at.%) of the Mg–La–Pd thin films measured by EDS.

	La 0.5 nm sample			La 2 nm sample			La 3 nm sample		
	Mg	La	Pd	Mg	La	Pd	Mg	La	Pd
Area A	78.6	0	21.4	74.6	1.2	24.2	74.5	4.0	21.5
Area B	72.3	2.8	24.9	74.7	2.5	22.8	71.0	3.9	25.1
Area C	73.8	2.7	23.3	72.7	3.7	23.6	72.4	4.0	23.6

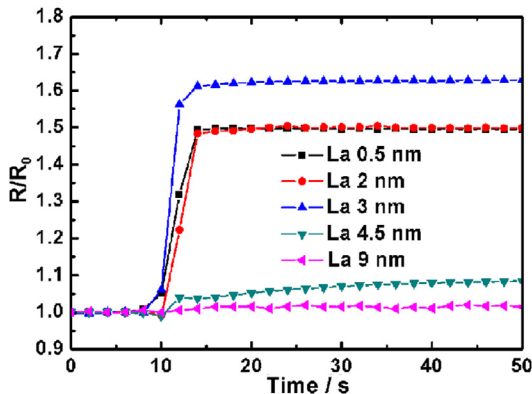


Fig. 2. The time evolution of the relative resistance, R/R_0 , of the Mg–La–Pd trilayer films under 0.1 MPa H_2 at 298 K.

14 s of hydrogenation, faster than the Mg/Ti/Pd film of 15 s [24] and Mg/Al/Pd film of 65 s [27], suggesting the complete transformation from Mg to MgH_2 . When the thickness of La is larger than 3 nm, the hydrogen absorption rate of the Mg–La–Pd films decreases with the increase of the La thickness. At the beginning of the hydrogenation, the Pd catalyst promotes the hydrogen dissociation and the hydride of PdH_x forms rapidly. Then, the hydrogen atoms pass through the hydride layer and diffuse in the metallic layer underneath [32]. We propose that in this work, the interlayer of La transforms into LaH_3 during hydrogenation, similar with other Mg-based nanomaterials containing La [33]. The thickness of the La layer is of great importance for the catalytic effect. When the La layer is very thin, e.g. 0.5 nm, the La layer is uneven and its catalytic effect on Mg hydrogenation/dehydrogenation can not be fulfilled. On the other hand, if the La layer is very thick, e.g. 9 nm, it will prohibit the diffusion of hydrogen toward Mg. The relative resistance of La 4.5 nm film reaches a constant value within 35 s of hydrogenation. As to the La 9 nm sample, the resistance value does not change for 50 s, suggesting that hydrogen atoms are blocked by the thick La interlayer. Thus, the La 3 nm sample exhibits the fastest hydrogen absorption kinetics at ambient temperature compared with other samples.

To examine the structural changes of La 3 nm sample during the hydrogenation and dehydrogenation, X-ray diffraction measurements were conducted and shown in Fig. 3 (a). The diffraction peaks around 40.0° are attributed to Pd (111). The as-prepared La 3 nm sample displays a diffraction peak around 34.6°

corresponding to the (002) plane of Mg. After hydrogenation at 298 K for 5 h, the Mg (002) peak in Fig. 3(b) disappears, whereas the MgH_2 (110) peak ($2\theta = 28.4^\circ$) can be clearly detected, indicating that the sample transforms completely from Mg into β - MgH_2 phase. After the full dehydrogenation in air at room temperature, the MgH_2 (110) peak disappears and the Mg (002) peak recovers, as shown in Fig. 3(c), suggesting a complete hydrogen adsorption–desorption cycle.

Fig. 4 (a) shows the optical transmittance spectra of the Mg–La–Pd trilayer films after absorbing 0.1 MPa H_2 at 298 K for 5 h. It is known that before hydrogenation, the Mg-based films are in the shiny metallic state and the transmittance values are close to zero [27]. It can be seen from Fig. 4 that after exposure to 0.1 MPa H_2 for 5 h, the transmittance values of the Mg–La–Pd samples increase due to the hydrogenation of the Mg layers, suggesting that all the samples can absorb hydrogen at room temperature. It is worth of noting that the transmittance value of the Mg–La–Pd film varies with the thicknesses of La interlayer, and the La 3 nm sample exhibits the largest transmittance value of 21.9%, higher than the Mg/Al/Pd film of 17% [27]. With the La thickness below 3 nm, the transmittance value increases with the La thickness, whereas it decreases when the La thickness is larger than 3 nm. This tendency agrees well with the resistance changes during the hydrogenation. The transmittance value of the La 9 nm sample is only about 0.05%. According to the Lambert–Beer law, the transmittance value can be correlated to the amount of hydrogen in the samples. It can be concluded that Mg in the La 3 nm sample transformed almost completely into MgH_2 phase, while the hydrogen atoms can hardly penetrate into the Mg layers in the La 9 nm sample due to the thick La interlayer. Fig. 4(b) displays the corresponding photographs of the La 3 nm sample during hydrogenation and desorption. The image of the camera is reflected by the as-prepared film before hydrogenation, so the badge of Beihang University behind the sample is unable to be observed. After hydrogenation at 298 K for 5 h, the whole badge is observed clearly through the transparent film, indicating a visible metal–insulator transition. After dehydrogenation in air at 298 K, the La 3 nm sample returns to the highly reflecting state and the badge is totally obscured again. The excellent switchable mirror properties can be potentially used in the hydrogen sensors and energy-efficient windows.

To evaluate the desorption kinetics of the La 3 nm sample, the optical transmittance changes of the La 3 nm sample at the wavelength of 500 nm, T/T_0 , with respect to exposure time during the desorption process at 298 K in air was measured and shown in Fig. 5. T_0 is the maximum transmittance of the film after full hydrogenation and T is the transmittance of the film during the desorption process. It is found that the transmittance value decreases immediately once the sample is exposed to air at room temperature, indicating the transition from the transparent hydride state to the highly reflecting metallic state. According to Lambert–Beer's law, $\ln(T/T_0)$, the logarithm of the optical transmittance is expected to vary linearly with the hydrogen concentration in the film [34]. The desorption rate can be determined from the slope of the curve, assumed that the sample is totally dehydrogenated when the transmittance reaches a constant value. Therefore, the amount of Mg hydride that transforms into Mg during the desorption process can be calculated. It is worth to note that the La 3 nm sample can release about 80% of the absorbed hydrogen within 60 min at room temperature.

Fig. 6 shows the cyclic voltammograms (CV) of the Mg–La–Pd films versus Hg/HgO electrode in 6 M KOH solution between -1.2 and 0.45 V. The broad cathodic wave in the CV curves around -1.0 V is assigned to the hydrogen absorption process, and the hydrogen evolution reaction occurs at potentials more negative than -1.0 V [35]. The broad anodic peak observed in the potential range of -0.5

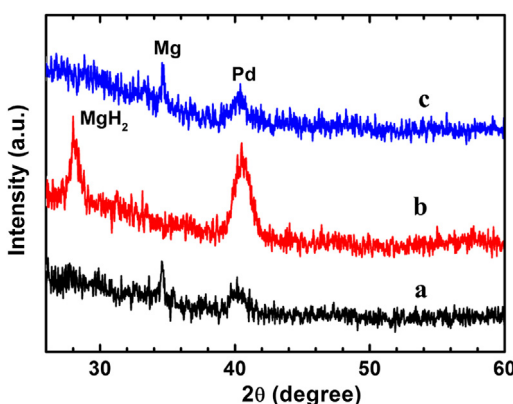


Fig. 3. XRD patterns of the Mg–La–Pd trilayer film with La interlayer of 3 nm: (a) as-prepared; (b) after hydrogenation in 0.1 MPa H_2 at 298 K for 5 h; (c) after dehydrogenation in air at 298 K for 5 h.

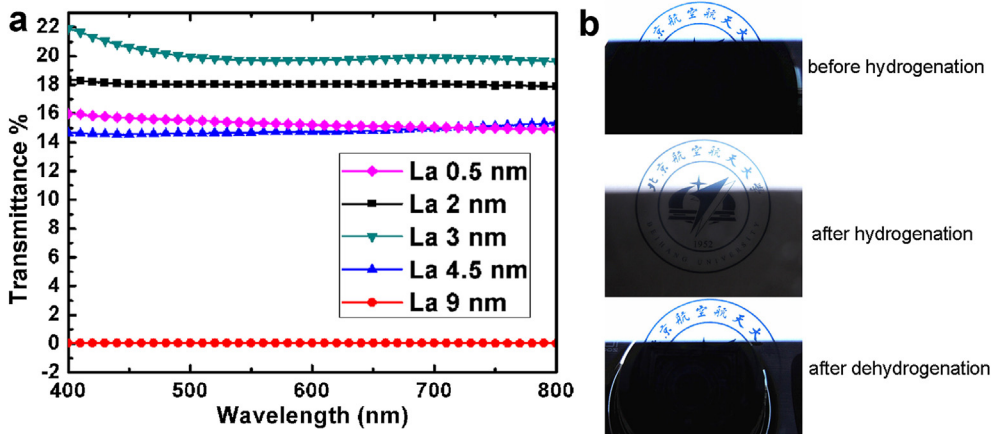


Fig. 4. (a) Optical transmittance spectra of the Mg–La–Pd trilayer films with various thickness after absorbing 0.1 MPa H₂ at 298 K for 5 h; (b) The corresponding photographs of the La 3 nm sample before hydrogenation, and after hydrogenation and dehydrogenation.

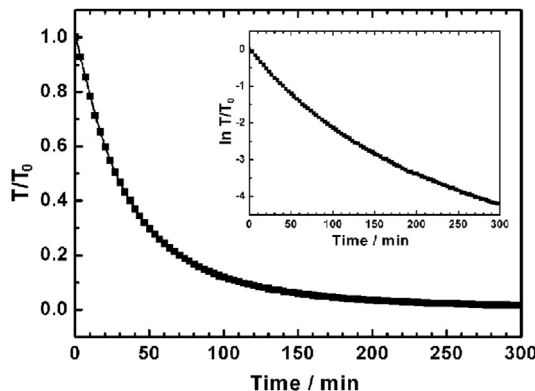


Fig. 5. The optical transmittance changes of the La 3 nm sample at wavelength of 500 nm, T/T_0 , with respect to exposure time during the desorption process at room temperatures in ambient air.

to -0.9 V is related to the hydrogen desorption [29]. The different locations of the anodic peaks are due to the different thicknesses of La interlayer in these samples. As shown in Fig. 6, the anodic area and anodic peak current density changes with the thickness of La interlayer at the same tendency with the resistance and the optical transmittance properties. The La 3 nm film possesses the largest

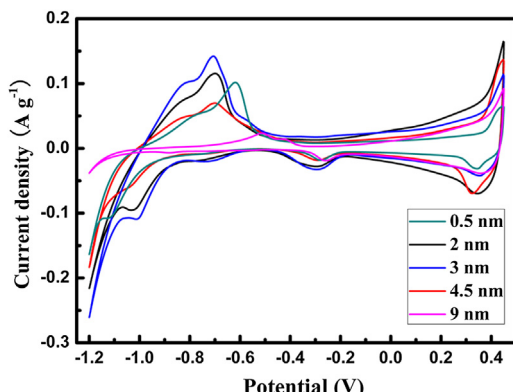


Fig. 6. The cyclic voltammograms (CV) of the Mg–La–Pd trilayer films versus Hg/HgO electrode in 6 M KOH solution between -1.2 and 0.45 V.

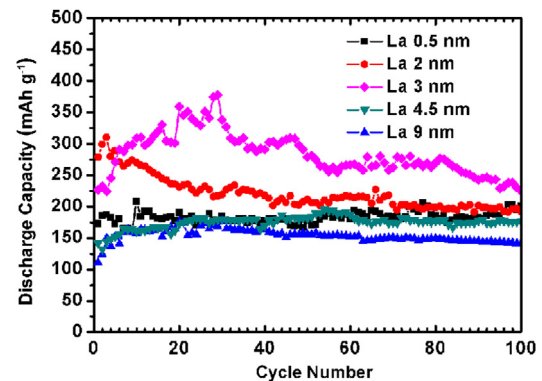


Fig. 7. The discharge capacity at different cycles of the Mg–La–Pd trilayer films.

anodic area and anodic peak current density of 0.1420 A g^{-1} , while the La 9 nm film has the smallest anodic area and anodic peak current density of 0.0227 A g^{-1} . It is well known that the value of peak current density can be used to evaluate the electrocatalytic activity of a hydride electrode. A larger peak current density means a higher electrocatalytic activity [36]. In this study, the large peak current density demonstrates a faster chemical reaction speed in the film electrode, which also means a faster hydrogen diffusion rate through the film. Therefore, hydrogen atoms diffuse much faster in the La 3 nm sample, compared with other films. This agrees well with the change of the electrical resistance of the Mg–La–Pd films during the hydrogen absorption shown in Fig. 2. This phenomenon can also be correlated to the thickness of La layer in the films. The hydrogen atoms can hardly diffuse to the surface of the Mg layer in case that the La interlayer is as thick as 9 nm.

The discharge capacities of the film can be determined by the amount of hydrogen absorbed and desorbed. Fig. 7 displays the discharge capacities at different cycles of the Mg–La–Pd films. It can be seen that the maximum discharge capacities of the La 0.5 nm, La 2 nm, La 3 nm, La 4.5 nm and La 9 nm are 207.8 , 310 , 377.8 , 195.1 and 175.7 mAh g^{-1} , respectively, exhibiting similar regularity with the electrical resistance changes of the Mg–La–Pd films during the hydrogen absorption. The La 3 nm sample displays the highest maximum discharge capacity among the Mg–La–Pd films, which is also quite larger than that of the La/Ni/Al film, about 220 mAh g^{-1} [30]. It is also found in Fig. 7 that the discharge

capacities of the Mg–La–Pd films decline only slightly after 100 cycles, showing a good cycle performance.

4. Conclusions

The Mg–La–Pd trilayer films with 0.5–9 nm La interlayer were prepared by magnetron sputtering method. With the increase of La layer thickness, the hydrogenation rate of the Mg–La–Pd films under 0.1 MPa H₂ at 298 K increases. The further increase of La layer thickness, larger than 3 nm, decreases the hydrogenation rate due to the prohibition of the continuous and thick La layer on the diffusion of H to the surface of Mg. The hydrogenation of the La 3 nm film saturates within 14 s, and it releases 80% of hydrogen within 60 min in air at room temperature, the fastest absorption/desorption kinetics compared with other Mg–La–Pd films. The electrochemical properties of the Mg–La–Pd films show similar trend to their hydrogen storage properties. The maximum discharge capacity of the La 3 nm film carried out in 6 M KOH is 377.8 mAh g^{−1}, the highest among these films, and it also shows a good cycle performance.

Acknowledgments

The authors acknowledge the support of this work by MOST of China (No. 2013CB035503, No. 2011AA03A408), China Program of Magnetic Confinement Fusion under grant number 2012GB102006, the Aeronautical Science Foundation of China (No. 2011ZF51065), and the Scientific Research Foundation for the Returned Overseas Chinese Scholars, State Education Ministry. We also thank Professor Huiping Duan and Center for Instrumental Analysis and Research, Beihang University for the technical aid in SEM observation.

References

- [1] B. Sakintuna, F. Lamari-Darkrim, M. Hirscher, *Int. J. Hydrogen Energy* 32 (2007) 1121–1140.
- [2] H.J. Cao, Y. Zhang, J.H. Wang, Z.T. Xiong, G.T. Wu, J.S. Qiu, P. Chen, *Dalt. Trans.* 42 (2013) 5524–5531.
- [3] Y. Wang, X. Wang, *Dalt. Trans.* 40 (2008) 5495–5500.
- [4] X.L. Wang, J.P. Tu, P.L. Zhang, X.B. Zhang, C.P. Chen, X.B. Zhao, *Int. J. Hydrogen Energy* 32 (2007) 3406–3410.
- [5] K.C. Hoffman, J.J. Reilly, F.J. Salzano, C.H. Waide, R.H. Wiswall, W.E. Winsche, *Int. J. Hydrogen Energy* 1 (1976) 133–151.
- [6] H. Imamura, K. Masanari, M. Kusuhara, H. Katsumoto, T. Sumi, Y. Sakata, *J. Alloys Compd.* 386 (2005) 211–216.
- [7] J.L. Bobet, E. Akiba, Y. Nakamura, B. Darriet, *Int. J. Hydrogen Energy* 25 (2000) 987–996.
- [8] K.J. Jeon, A. Theodore, C.Y. Wu, *J. Power Sources* 183 (2008) 693–700.
- [9] W.P. Kalisvaart, C.T. Harrower, J. Haagsma, B. Zahiri, E.J. Luber, C. Ophus, E. Poirier, H. Fritzsche, D. Mitlin, *Int. J. Hydrogen Energy* 35 (2010) 2091–2103.
- [10] X.H. Tan, C.T. Harrower, B.S. Amirkhiz, D. Mitlin, *Int. J. Hydrogen Energy* 34 (2009) 7741–7748.
- [11] T. Liu, C.G. Qin, T.W. Zhang, Y.R. Cao, M. Zhu, X.G. Li, *J. Mater. Chem.* 22 (2012) 19831–19838.
- [12] B. Dam, R. Gremaud, C. Broedersz, R. Griessens, *Scr. Mater.* 56 (2007) 853–858.
- [13] M. Suzuki, T. Tanaka, K. Kawabata, *Thin Solid Films* 343 (1999) 21–23.
- [14] S. Singh, S.W.H. Eijt, M.W. Zandbergen, W.J. Legerstee, V.L. Svetchnikov, *J. Alloys Compd.* 441 (2007) 344–351.
- [15] A. Ludwig, J. Cao, B. Dam, R. Gremaud, *Appl. Surf. Sci.* 254 (2007) 682–686.
- [16] L. Pranevicius, E. Wirth, D. Milcicus, M. Lelis, L.L. Pranevicius, A. Kanapickas, *Surf. Coat. Technol.* 203 (2009) 998–1003.
- [17] T.J. Richardson, J.L. Slack, R.D. Armitage, R. Kostecki, B. Farangis, M.D. Rubin, *Appl. Phys. Lett.* 78 (2001) 3047–3049.
- [18] Y.M. Tang, C.W. Ong, *J. Mater. Res.* 24 (2009) 1928–1935.
- [19] H. Wang, L.Z. Ouyang, M. Zeng, M. Zhu, *Int. J. Hydrogen Energy* 29 (2004) 1389–1392.
- [20] R. Gremaud, C.P. Broedersz, D.M. Borsa, A. Borgschulte, P. Mauron, H. Schreuders, J.H. Rector, B. Dam, R. Griessens, *Adv. Mater.* 19 (2007) 2813–2817.
- [21] J.L. Xu, D. Niu, Y.J. Fan, *J. Power Sources* 198 (2012) 383–388.
- [22] J.L. Qu, Y.T. Wang, L. Xie, J. Zheng, Y. Liu, X.G. Li, *J. Power Sources* 186 (2009) 515–520.
- [23] J.L. Qu, B. Sun, J. Zheng, R. Yang, Y.T. Wang, X.G. Li, *J. Power Sources* 195 (2010) 1190–1194.
- [24] G.B. Xin, J.Z. Yang, C.Y. Wang, J. Zheng, X.G. Li, *Dalt. Trans.* 41 (2012) 6783–6790.
- [25] L.Z. Ouyang, H. Wang, C.Y. Chung, J.H. Ahn, M. Zhu, *J. Alloys Compd.* 422 (2006) 58–61.
- [26] Z. Tan, C. Chiu, E.J. Heilweil, L.A. Bendersky, *Int. J. Hydrogen Energy* 36 (2011) 9702–9713.
- [27] G.B. Xin, J.Z. Yang, G.Q. Zhang, J. Zheng, X.G. Li, *Dalt. Trans.* 41 (2012) 11555–11558.
- [28] B. Zahiri, C.T. Harrower, B.S. Amirkhiz, D. Mitlin, *Appl. Phys. Lett.* 95 (2009) 103114.
- [29] D.K. Slattery, *Int. J. Hydrogen Energy* 20 (1995) 971–973.
- [30] C.Y.V. Li, Z.M. Wang, S. Liu, S.L.I. Chan, *J. Alloys Compd.* 456 (2008) 407–412.
- [31] P. Hjort, A. Krozer, B. Kasemo, *J. Alloys Compd.* 237 (1996) 74–80.
- [32] J.L. Qu, B. Sun, Y. Liu, R. Yang, Y.Q. Li, X.G. Li, *J. Hydrogen Energy* 35 (2010) 8331–8336.
- [33] T. Liu, C.G. Qin, M. Zhu, Y.R. Cao, H.L. Shen, X.G. Li, *J. Power Sources* 219 (2012) 100–105.
- [34] M. Pasturel, M. Slaman, H. Schreuders, J.H. Rector, D.M. Borsa, B. Dam, R. Griessens, *J. Appl. Phys.* 100 (2006) 023515.
- [35] J. Paillier, S. Bouhtiyya, G.G. Ross, L. Roué, *Thin Solid Films* 500 (2006) 117–123.
- [36] J. Paillier, L. Roué, *J. Alloys Compd.* 404 (2005) 473–476.